

Pedotransfer functions for estimating saturated hydraulic conductivity of selected benchmark soils in Ghana

ABSTRACT

Aims: Direct methods of measuring saturated hydraulic conductivity (K_s), either in situ or in the laboratory, are time consuming and very expensive. Several Pedotransfer functions (PTFs) are available for estimating K_s , with each having its own limitations. In this study, the performances of four popular PTFs were evaluated on different soil classes. The PTFs considered herein were Puckett et al. (1985), Campbell and Shiozawa (1994), Dane and Puckett (1994), and Ferrer-Julià et al. (2004). In addition, five local data derived PTFs were used to study the possibility of using local datasets to validate PTF accuracy.

Materials and methods: A total of 450 undisturbed soil cores were collected from the 0 – 15 cm depth from a Stagni-Dystric Gleysol (SDG), Plinthis Ferric Acrisol (PFA) and Plinthic Acrisol (PA). The K_s of samples were measured by falling-head permeameter method in the laboratory. Sand, silt and clay fractions, bulk density, organic matter content, and exchangeable calcium and sodium were measured and used as input parameters for the derived PTFs. Accuracy and reliability of the predictions were evaluated by the root mean square error (RMSE), coefficient of correlation (r), index of agreement (d), and the Nash-Sutcliffe efficiency (NSE) between the measured and predicted values. The relative improvement (R) of the derived PTFs from this study over the existing ones were also evaluated.

Results: The derived PTFs in this study had good prediction accuracy with r , d , RMSE and NSE ranging from 0.80 – 0.99, 0.79 – 0.94, 0.14 – 1.74 and 0.84 – 0.98, respectively, compared with 0.32 – 0.45, 0.27 – 0.50, 4.00 – 4.90 and 0.41 – 0.47 for the tested PTFs. The relative improvement of the derived over the tested PTFs ranged from 56.50 – 95.71% in the SDG, 70.73 – 96.89% in the PFA, and 65.37 – 95.81% in the PA. Generally, R was observed to be highest for Model 1 in the SDG, and Model 4 in both PFA and PA, and lowest for Model 5 in all three soils. It was observed that the inclusion of exchangeable calcium and sodium as predictors increased the predictability of the derived PTFs.

Keywords: Clay, Pedotransfer function, Saturated hydraulic conductivity, Sand

1. INTRODUCTION

Hydraulic conductivity is a major parameter in all hydrological models, spanning from physically-based, fully-distributed small-catchment models to land surface parameterizing schemes of general circulation or global climate models [1, 2]. Hydraulic conductivity in saturated soils, referred to as the saturated hydraulic conductivity (K_s) is very crucial in soil and water management with regard to ecology, agriculture and the environment [3, 4]. In addition, it is a very significant parameter in the study of processes such as infiltration, irrigation and drainage, runoff and erosion, and heat and mass transport in top soils, and solute transport in soils [5 – 7]. However, direct determination of K_s under both field and laboratory conditions can be very tedious, time constraining, and cost inefficient, especially over large scales [8], and may often result in unreliable data due to soil heterogeneity and experimental errors. As a result, indirect methods often adopted estimate K_s from other soil

25 properties. These are categorized into three, namely, pore-size distribution models, inverse
26 methods, and pedotransfer functions [1, 9].

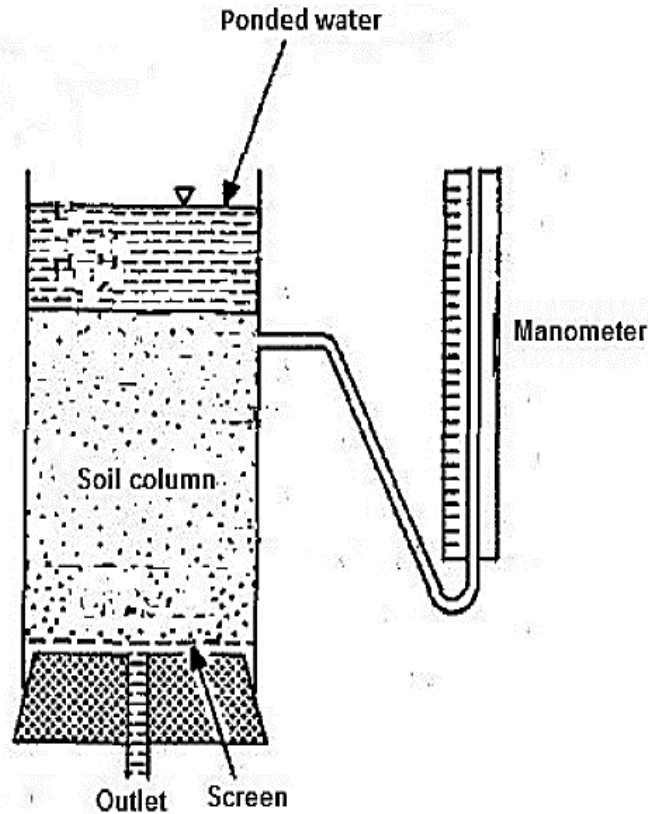
27 Pedotransfer functions are mainly empirical; however, physico-empirical models and fractal
28 theory models are also available [10]. They are generally employed for estimating hydraulic
29 properties from soil properties such as soil texture, bulk density, organic matter content, and
30 water retention [1, 10, 11]. According to Schaap [11] any PTF may belong to one of three
31 main groups, namely, Class PTFs, Continuous PTFs, and Neural network analysis-derived
32 PTFs. The Class PTFs [e.g. 12 – 14] are based on the similar media theory [15], wherein,
33 similar soils are assumed to exhibit similar hydraulic properties. Continuous PTFs, which are
34 mainly derived from linear and nonlinear regression models, show a continuous trend of
35 variations among estimated hydraulic properties for defined textural classes [16]. All PTFs
36 are developed from data obtained from a small number of soil samples, and usually do not
37 account for soil structural heterogeneities, which may result in less accurate or poor
38 predictions when applied to soils different from those from which they were developed [7,
39 17]. This implies that the prediction accuracy of PTFs depends on the similarity between the
40 soils from which they were developed and tested [18]. Inclusion of extra basic soil
41 properties, such as bulk density, porosity, organic matter content, water retention
42 parameters [19 – 22], and exchangeable sodium and calcium may improve the prediction
43 performance of such models. It is therefore, important to evaluate how well PTFs will
44 perform when applied outside the range of the data that were used to derive them, and to
45 make appropriate modifications where necessary. The objectives of the study were to:

- 46 i. Evaluate the general reliability of four most commonly cited PTFs to predict K_s of
47 selected Ghanaian soils, where climatic and geological conditions are different from
48 where they were developed and tested;
- 49 ii. Derive and verify, for selected benchmark soils in Ghana, more accurate PTFs to
50 estimate K_s ;
- 51 iii. Test whether the inclusion of exchangeable Na and Ca as input parameters would
52 improve the accuracy of the derived PTFs.

53 **2. MATERIAL AND METHODS**

54 **2.1 Soil sampling, analysis and characterization**

55 A set undisturbed soil samples were collected from the surface 0 – 15 cm depth with a core
56 sampler of 10 cm diameter and 30 cm height. The soils were classified as Stagni-Dystric
57 Gleysol (SDG), Plinthi Ferric Acrisol (PFA) and Plinthic Acrisol (PA). In total, 450
58 undisturbed cores and two sets of 450 disturbed samples were collected. One set of the
59 disturbed samples was oven-dried and used for the determination of bulk density; the other
60 set was air-dried and sieved through a 2 mm sieve. The disturbed samples were used for
61 the determination of particle size distribution, pH, organic matter content, exchangeable
62 sodium, calcium, magnesium, and potassium, cation exchange capacity, exchangeable
63 sodium percentage and sodium absorption ratio. The undisturbed cores were used for the
64 laboratory measurements of saturated hydraulic conductivity. Soil bulk density was
65 estimated based on the weight of soil core samples after correcting for soil moisture and the
66 mass and volume of roots and stones [23]. Saturated moisture content was assumed to be
67 equal to the total porosity [24, 25]. Particle size analysis was determined by the hydrometer
68 method. The saturated hydraulic conductivity was determined on laboratory soil columns
69 with the falling head permeameter (Figure 1) [2, 26]. Measured properties of the soil classes
70 are presented in Table 1. The soil textures were sandy, sandy loam, and loamy sand.



71

72 **Figure 1.** Laboratory setup for the determination of saturated hydraulic conductivity
 73 Source: Tuffour et al. [27]

74 **2.1.1 Collection of soil cores**

75 Soil sampling was done as described by Tuffour [2]. Undisturbed soil cores were collected
 76 from the fields using a 10 cm diameter PVC pressure sewer pipe and a height of 30 cm and
 77 beveled on the outer part of one end to provide a cutting edge to facilitate the insertion of
 78 the core. Soil cores were collected by first digging a circular trench around an intact "pillar"
 79 of undisturbed soil which was taller and had a slightly larger diameter than the core sampler.
 80 The core sampler was then inserted directly into the pillar of soil by striking a wooden plank
 81 positioned across the top of the ring, with a mallet. By this, the edges of the pillar were
 82 allowed to fall away from the core as it was inserted. Following complete insertion, the core
 83 was excavated by hand. A sealant (herein, paraffin wax) was used to ensure good contact
 84 between the soil and core, and thereby minimised any edge flow resulting from an air
 85 annulus created by the inner ring down the core.

86 **2.1.2 Determination of saturated hydraulic conductivity**

87 Determination of K_s was done as described by Tuffour [2]. Undisturbed soil cores samples
 88 were soaked for 24 hours in water until they were completely saturated. The saturated core
 89 was gently placed on gravel supported by a plastic sieve. The set up was placed in a sink,
 90 and water was gently added to give hydraulic head in the extended cylinder. The fall of the
 91 hydraulic head (h_t) on the soil surface was measured as a function of time (t) using a water
 92 manometer with a 5-meter scale (Figure 1). Saturated hydraulic conductivity was calculated
 93 by the standard falling head equation given as:

$$K_s = \left(\frac{aL}{At} \right) \ln \left(\frac{h_o}{h_t} \right); \quad (1)$$

94 where,

95 a = Surface area of the cylinder [L^2]

96 A = Surface area of the soil [L^2]

97 h_o = Initial hydraulic head [L]

98 L = Length of the soil column [L]

99 h_t = Hydraulic head after a given time t [L]

100 Rewriting equation (1), a regression of $\ln\left(\frac{h_o}{h_t}\right)$ on t with slope $b = K_s \left(\frac{A}{La}\right)$ was obtained.

101 Since $a = A$ in this particular case, K_s was simply calculated as:

$$K_s = bL \quad (2)$$

102 Samples of measurement data on soil properties from the study are presented in the
103 following Tables 1 – 3.

104 **Table 1.** Example data of soil properties of the Stagni-Dystric Gleysol

Sample	Soil property								
	Sand (%)	Silt (%)	Clay (%)	Texture	BD (g/cm^3)	OM (%)	Na (cmol/kg)	Ca (cmol/kg)	K_s (cm/min)
1	83.52	8.88	7.60	LS	1.62	0.83	0.040	1.6	0.30
2	87.48	7.32	5.20	LS	1.62	1.24	0.116	1.6	0.18
3	93.52	1.68	4.80	S	1.48	0.28	0.040	1.4	0.47
4	94.37	1.15	4.48	S	1.32	0.14	0.040	1.8	0.59
5	91.52	3.60	4.88	S	1.34	0.48	0.040	1.2	0.39
6	87.6	6.80	5.60	LS	1.34	1.03	0.040	2.2	0.95
7	91.52	3.20	5.28	S	1.57	1.03	0.040	1.0	0.15
8	91.52	3.28	5.20	S	1.52	0.62	0.040	1.0	0.035
9	81.52	13.20	5.28	LS	1.58	0.34	0.040	1.8	0.62
10	87.60	6.64	5.76	LS	1.56	0.32	0.040	1.4	0.83
11	91.52	3.60	4.88	S	1.56	0.34	0.040	1.6	0.18
12	87.48	7.08	5.44	LS	1.70	0.62	0.040	1.2	0.12
13	85.32	9.28	5.40	LS	1.47	0.41	0.040	1.6	0.21
14	92.44	2.48	5.08	S	1.34	0.14	0.040	1.6	0.24
15	92.44	2.76	4.80	S	1.55	0.89	0.040	1.6	0.027

105 BD = Bulk density; K_s = Saturated hydraulic conductivity; OM = Organic matter; Na and Ca =
106 Exchangeable sodium and calcium; LS = Loamy sand; S = Sand

107

108

109

110

111

112

113

114 **Table 2.** Example data of soil properties of the Plinthi Ferric Acrisol

Sample	Soil property								
	Sand (%)	Silt (%)	Clay (%)	Texture	BD (g/cm ³)	OM (%)	Na (cmol/kg)	Ca (cmol/kg)	K _s (cm/min)
1	86.46	8.56	4.98	LS	1.24	4.47	0.040	5.4	1.50
2	90.38	4.56	5.06	S	1.39	3.64	0.040	6.4	1.20
3	92.60	2.34	5.06	S	1.34	4.47	0.040	8.0	1.32
4	82.38	8.56	9.06	LS	1.38	3.58	0.040	6.6	1.56
5	86.38	6.56	7.06	LS	1.54	3.50	0.040	8.0	0.15
6	82.38	10.56	7.06	LS	1.37	4.53	0.040	8.2	1.47
7	88.38	4.49	7.13	LS	1.38	4.12	0.040	8.0	0.39
8	88.38	6.49	5.13	S	1.50	3.64	0.040	7.0	1.37
9	86.38	6.56	7.06	LS	1.37	3.85	0.040	7.8	0.78
10	84.31	6.49	9.20	LS	1.39	4.05	0.040	7.8	0.90
11	84.67	4.99	10.34	LS	1.46	3.44	0.040	7.4	0.42
12	84.67	6.99	8.34	LS	1.48	2.88	0.040	9.0	0.71
13	84.67	8.99	6.34	LS	1.41	3.85	0.040	7.2	0.80
14	82.67	8.99	8.34	LS	1.50	3.30	0.040	8.0	1.56
15	86.67	4.92	8.41	LS	1.41	3.23	0.040	5.4	1.16

115 BD = Bulk density; K_s = Saturated hydraulic conductivity; OM = Organic matter; Na and Ca =
 116 Exchangeable sodium and calcium; LS = Loamy sand; S = Sand

117 **Table 3.** Example data of soil properties of the Plinthic Acrisol

Sample	Soil property								
	Sand (%)	Silt (%)	Clay (%)	Texture	BD (g/cm ³)	OM (%)	Na (cmol/kg)	Ca (cmol/kg)	K _s (cm/min)
1	84.40	8.84	6.76	LS	1.23	1.99	0.040	7.6	0.84
2	82.44	10.88	6.68	LS	1.30	1.85	0.040	4.8	0.65
3	82.44	10.72	6.84	LS	1.36	2.41	0.040	6.0	0.80
4	84.44	8.80	6.76	LS	1.23	2.06	0.0019	4.0	1.19
5	75.16	10.56	14.28	SL	1.26	2.41	0.0019	4.2	1.44
6	80.52	12.64	6.84	LS	1.29	2.20	0.040	6.2	1.13
7	85.60	8.56	5.84	LS	1.48	3.02	0.0019	4.6	1.52
8	85.60	8.56	5.84	LS	1.057	2.47	0.040	2.0	1.58
9	87.60	6.48	5.92	LS	1.13	1.31	0.040	4.8	1.23
10	81.16	8.56	10.28	LS	1.31	3.02	0.040	6.2	2.36
11	83.60	6.48	9.92	LS	1.11	2.61	0.0019	5.2	1.20
12	83.60	8.48	7.92	LS	1.13	2.34	0.040	4.4	0.80
13	87.52	6.56	5.92	LS	1.13	3.23	0.0019	4.4	1.67
14	83.16	10.64	6.20	LS	1.021	2.42	0.0019	3.8	0.41
15	85.24	8.48	6.28	LS	1.048	2.68	0.0019	4.8	2.97

118 BD = Bulk density; K_s = Saturated hydraulic conductivity; OM = Organic matter; Na and Ca =
 119 Exchangeable sodium and calcium; LS = Loamy sand; SL = Sandy loam

120 **2.2 Pedotransfer functions (PTFs)**

121 Saturated hydraulic conductivity was predicted by relating it to basic soil properties using
 122 PTFs. The commonly cited PTFs evaluated were those developed by Puckett et al. [28],
 123 Campbell and Shiozawa [29], Dane and Puckett [30], and Ferrer-Julιά et al. [31] as
 124 presented in equations (3 – 6), respectively:

125
$$K_s = 156.96 \exp[-0.1975C_l] \quad (3)$$

126
$$K_s = 54 \exp[-0.07S_a - 0.167C_l] \quad (4)$$

127 $K_s = 303.84 \exp(-0.144C_l)$ (5)

128 $K_s = 2.556 \times 10^{-7} \exp(0.0491S_a)$ (6)

129 Additionally, five new PTFs, (Equations 7 – 11), were derived using multiple linear
 130 regression (MLR) to relate K_s to particle size distribution, bulk density, exchangeable sodium
 131 and cation, and organic matter content. The derived PTFs (Equations 7 – 11) in this study
 132 are:

133 Model 1: $K_s = 0.046158S_a + 0.008362S_i + 0.107176Ca - 1.121352Na$ (7)

134 Model 2: $K_s = 0.02256S_i + 0.06784C_l + 0.29335OM + 0.14592Ca + 33.75189Na$ (8)

135 Model 3: $K_s = 0.1832C_l + 40.9297Na$ (9)

136 Model 4: $K_s = 2.743BD + 1.123Na$ (10)

137 Model 5: $K_s = 0.45615Ca + 37.403333Na$ (11)

138 where, K_s = Saturated hydraulic conductivity [L/T]; S_a = Sand content; S_i = Silt content; C_l =
 139 Clay content; BD = Bulk density; OM = Organic matter; Na = Exchangeable sodium; Ca =
 140 Exchangeable calcium

141 The first model (Model 1) uses sand, silt percentages, and exchangeable calcium and
 142 sodium contents. The second model (Model 2) uses silt and clay percentages, organic
 143 matter, and exchangeable calcium and sodium contents. The third model (Model 3) uses
 144 clay percentage and exchangeable sodium content. The fourth model (Model 4) uses bulk
 145 density and exchangeable sodium content. The fifth model (Model 5) uses exchangeable
 146 calcium and sodium contents.

147 2.3 Performance evaluation of the PTFs

148 In order to evaluate the performance of the PTFs in predicting K_s , the K_s values estimated
 149 from the derived and tested PTFs were compared to the laboratory measured K_s values,
 150 and assessed with the root mean square error (RMSE) (Equation 12), index of agreement
 151 (d) (Equation 13), correlation coefficient (r) (Equation 14), relative improvement (R)
 152 (Equation 15), and Nash–Sutcliffe efficiency (NSE) (Equation 16). The d statistic was used
 153 to avoid problems related with coefficient of determination (R^2).

$$RMSE = \left[\frac{1}{n} \sum_{i=1}^n (d_s - d_o)_i^2 \right]^{1/2} \quad (12)$$

$$d = 1 - \left(\frac{\sum_{i=1}^n (d_s - d_o)_i^2}{\sum_{i=1}^n [(d_s - \bar{d}_o)_i + (d_o - \bar{d}_o)_i]^2} \right) \quad (13)$$

154 where, n = Number of observations; d_o = Observed data; d_s = Simulated data

$$r = \sqrt{1 - \frac{SSE}{SST}} \quad (14)$$

155 where, SSE measures the deviations of observations from their predicted values and SST is
 156 a measure of the deviations of the observations from their mean.

$$RI = \left(\frac{RMSE_E - RMSE_D}{RMSE_E} \right) \times 100 \quad (15)$$

157 where, $RMSE_E$ = $RMSE$ of the existing models; $RMSE_D$ = $RMSE$ of the derived models

158 The Nash–Sutcliffe efficiency was estimated as:

$$NSE = 1 - \left[\frac{\sum_{i=1}^n (d_s - d_o)^2}{\sum_{i=1}^n (d_s - \bar{d}_o)^2} \right] \quad (16)$$

159 where, d_s = Calculated values of K_s ; d_o = Observed values of K_s ; n = Number of
160 observations

161 3. RESULTS AND DISCUSSION

162 Saturated hydraulic conductivity was estimated from the above-mentioned PTFs, and
163 compared to measured K_s of the 45 spots in each study site. The performance of the tested
164 PTFs were assessed based on the quality of the estimations when applied on specific soil
165 data from this study. However, since those PTFs were developed from different soil
166 datasets, their predictability is always expected to be dependent on the set from which they
167 were developed and those on which they are tested [18]. The results of scatter plots of
168 measured versus estimated K_s for the derived and tested PTFs, and their performance
169 statistics are presented in **Table 4**. The input data required for the PTFs varied upon the
170 parameters used in developing a particular model. This resulted in variations in their
171 performances in the prediction of K_s . In general, the performances of the well-known PTFs
172 were not good as evidenced by the evaluation indices (i.e., r , d , RMSE and NSE) as shown
173 in **Table 4**. This implies that no particular model amongst the well-known PTFs could be said
174 to have yielded the best quality fit for K_s in this study. However, estimated K_s by from the
175 PTFs showed a positive correlation with measured K_s . Generally, the r values observed in
176 the study were comparable to those reported by Agyare et al. [32], who reported r in the
177 range of 0.29 – 0.41 when NN model, a concept that is very similar to PTF was used to
178 estimate K_s .

179 **Table 4. Goodness-of-fit indicators for the well-known PTFs**

Soil	Equation	r	RMSE	d	NSE
Stagni-Dystric Gleysol	P	0.40	4.00	0.45	0.42
	CS	0.35	4.10	0.44	0.41
	DP	0.35	4.90	0.44	0.46
	FJ	0.35	4.30	0.40	0.43
Plinthi Ferric Acrisol	P	0.45	4.10	0.50	0.47
	CS	0.40	4.30	0.39	0.44
	DP	0.43	4.20	0.40	0.44
	FJ	0.41	4.50	0.27	0.46
Plinthic Acrisol	P	0.38	4.10	0.32	0.40
	CS	0.32	4.30	0.36	0.45
	DP	0.32	4.20	0.45	0.42
	FJ	0.32	4.10	0.37	0.44

180 r = Correlation coefficient; RMSE = Root mean square error; d = Index of agreement; P =
181 Puckett et al. [28]; CS = Campbell and Shiozawa [29]; DP = Dane and Puckett [30]; FJ =
182 Ferrer-Julìa et al. [31]; NSE = Nash–Sutcliffe efficiency

183
184 Since the ultimate goal of this study was to find a suitable PTF to include in soil water
185 management scheduling, it was imperative to also develop PTFs upon the failure of the

186 tested ones (Table 4) to predict K_s . A key aspect of this study, therefore, dealt with the
 187 identification of additional soil information that could improve the accuracy of the PTFs,
 188 besides the traditional PTF predictors, viz., sand, silt, and clay contents, bulk density, and
 189 OM content. This implies that PTF development should be site-specific [33, 34]. From the
 190 set of derived PTFs, OM was only applicable in Model 2, even though it was listed among
 191 the essential input parameters to build PTFs in this study. A possible reason, according to
 192 Tomasella et al. [35] is that not only the quantity, but the quality of organic matter
 193 significantly affects soil hydraulic properties. In addition, OM is reported to be an important
 194 variable for estimating unsaturated soil hydraulic properties; it has less effect in saturated
 195 soils, since OM mainly affects retention forces (matric potential), which are ca. zero in
 196 saturated soils [36, 37]. Also, the exchangeable Na and Ca contents, and bulk density made
 197 the use of OM unnecessary. Thus, the use of bulk density [35, 38], and exchangeable Na
 198 and Ca were effective substitutes for OM in the development of PTFs in this study.
 199

200 Table 5 presents the performance indices of the derived PTFs. While the performances of
 201 all the well-known PTFs were generally poor, those of the derived PTFs (Models 1 – 5) were
 202 highly accurate, as revealed by the very high r , d , NSE, and very low RMSE values.
 203 Contrary to the tested the PTFs, Models 1 – 5 would allow for the assessment of changes in
 204 OM, bulk density [39], and exchangeable Na and Ca on K_s . Compared to the best predictor
 205 amongst the well-known PTFs, herein, Puckett et al. [28] model with RMSE between 4.00
 206 and 4.10, the derived PTFs provided high accuracy, with RMSE not exceeding 1.741. In
 207 addition, the NSE values of the derived PTFs ranged between 0.844 – 0.950 in the SDG,
 208 0.854 – 0.982 in the PFA, and 0.892 – 0.972 in the PA. This implies that the PTFs
 209 developed from the local datasets had a superior performance over the well-known ones.
 210 The relatively poor prediction of the well-known PTFs may be explained by the selection of
 211 inappropriate soil properties as predictors [40]. This corroborates the reports by several
 212 studies [e.g. 5, 41 – 43] that the performance of PTFs is highly affected by factors such as
 213 geographical source of data used for its derivation, and differences in methods of
 214 measurement. Additionally, according to Tuffour [2], most theories in soil hydrology,
 215 including these well-known PTFs have been developed for standard, clay-rich and organic-
 216 rich, and fertile temperate soils. This implies that these models are generally successful for
 217 moist environments, but do not always carry over meaningfully over arid and semi-arid
 218 regions as in the present study. The derived PTFs, on the other hand, are a simple and
 219 suitable approach for the determination of K_s in the absence of instrumentation.
 220

221 **Table 5. Goodness-of-fit indicators for the derived PTFs**

Soil	Equation	r	RMSE	d	NSE
Stagni-Dystric Gleysol	Model 1	0.892	0.213	0.794	0.844
	Model 2	0.994	0.584	0.920	0.932
	Model 3	0.993	1.040	0.911	0.950
	Model 4	0.994	0.283	0.923	0.873
	Model 5	0.991	1.741	0.874	0.931
Plinthi Ferric Acrisol	Model 1	0.990	0.154	0.893	0.982
	Model 2	0.993	0.212	0.941	0.963
	Model 3	0.991	0.714	0.844	0.940
	Model 4	0.994	0.143	0.921	0.903
	Model 5	0.992	1.204	0.873	0.854
Plinthic Acrisol	Model 1	0.971	0.203	0.863	0.892
	Model 2	0.992	0.534	0.922	0.930
	Model 3	0.991	0.670	0.874	0.952
	Model 4	0.993	0.181	0.911	0.894
	Model 5	0.991	1.422	0.912	0.972

222 r = Correlation coefficient; RMSE = Root mean square error; d = Index of agreement; NSE =
 223 Nash–Sutcliffe efficiency
 224

225 The observation made in the study is a clear evidence of inter-user variability emanating
 226 from soil surface characteristics, presence of a protective layer, and land use history of the
 227 study site [44] and site specificity of PTFs, which are the key limitations of applying PTFs
 228 developed in one region to other regions [45, 46]. Hence, the prediction of K_s using PTFs
 229 could be well improved by adding input variables such as topographic, vegetation, and land
 230 use and/or by enlarging the datasets [47]. This clearly shows the importance of using local
 231 data in the development of K_s PTFs as corroborated by [46], who assessed the
 232 performances of four PTFs (Jabro, Puckett, Neurotheta, and Rosetta) with a locally derived
 233 PTF (Turkey). They reported the lowest RMSE value of 0.74 for the Turkey against Rosetta,
 234 which performed best among the four well-known PTFs, with RMSE of 1.61. The index of
 235 agreement (d) (Table 5), ranged between 0.79 (for Model 1 in the SDG) and 0.94 (for Model
 236 2 in the PFA), which reflects reasonable performance of the derived PTFs. The d statistic
 237 herein reflects the degree to which the observations were accurately estimated by the
 238 predictions [43, 48]. In all, the results indicate very good performance of the derived PTFs in
 239 terms of the four statistics used as evaluation indices.

240
 241 As presented in Table 6, the addition of Ca and Na as input parameters for the derived
 242 PTFs improved the predictions of K_s between 57.56% and 95.71% in the SDG, 70.73% and
 243 96.89% in the PFA, and 65.37% and 95.81% in the PA. Most especially, it was found that K_s
 244 was directly affected by exchangeable Na, which was in fact the most important soil property
 245 influencing K_s in the soils in this study. The performances of the derived PTFs based on
 246 their relative improvements over the well-known ones were in the order of Model 1 > Model
 247 4 > Model 2 > Model 3 > Model 5 for the SDG, and the PFA, and Model 4 > Model 1 >
 248 Model 2 > Model 3 > Model 5 for the PA. The large improvement may be attributed to the
 249 consideration of additional properties, particularly Na as input parameters. The PTF with OM
 250 as an input variable (Model 2) performed very well in estimating K_s as reported by Wösten
 251 [13] and Vereecken et al. [20]. Similar to fine textured soils as reported by Candemir and
 252 Gülser [49], K_s depends on both soil physical and chemical properties in coarse textured
 253 soils. The differences in the results between estimates from the derived and tested PTFs
 254 may not be exclusively due to the inclusion of OM, exchangeable Ca and Na, but also from
 255 other factors such as database-related uncertainties and the adopted algorithms [9, 44, 50].
 256
 257

Table 6. Relative improvement of the derived over the tested PTFs

Soil	Equation	Relative Improvement (%)			
		P	CS	DP	FJ
Stagni-Dystric Gleysol	Model 1	94.75	94.88	95.71	95.12
	Model 2	85.50	85.85	88.16	86.51
	Model 3	74.00	74.63	78.78	75.81
	Model 4	93.00	93.17	94.29	94.65
	Model 5	56.50	57.56	64.49	59.53
Plinthi Ferric Acrisol	Model 1	96.34	96.51	96.43	96.67
	Model 2	94.88	95.11	95.00	95.33
	Model 3	82.68	83.49	83.10	84.22
	Model 4	96.59	94.74	96.67	96.89
	Model 5	70.73	72.09	71.43	73.33
Plinthic Acrisol	Model 1	95.12	95.35	95.24	95.12
	Model 2	87.07	87.67	87.38	87.07
	Model 3	83.66	84.42	84.05	83.66
	Model 4	95.61	95.81	95.71	95.61
	Model 5	65.37	66.98	66.19	65.37

258 P = Puckett *et al* [28]; CS = Campbell and Shiozawa [29]; DP = Dane and Puckett [30]; FJ =
 259 Ferrer-Julià *et al* [31]
 260
 261

4. CONCLUSION

262 This study tested the application of four well-known Pedotransfer Functions (PTFs) in the
263 literature and local data derived PTFs, to identify the level of accuracy to estimate K_s for
264 some selected benchmark soils in Ghana. Multilinear regression analysis was used to derive
265 the best relationships between K_s and some basic soil properties. The derived PTFs
266 provided more accurate predictions, whereas the well-known PTFs underestimated K_s
267 values for all three soil types. The derived PTFs in this study are highly advantageous over
268 the tested ones due to the overall low error levels (i.e., higher r , d and NSE values, and
269 lower RMSE values) and simplicity to input parameters. Reliability of the developed PTFs
270 (Models 1 – 5) against the well-known ones demonstrated the ability of the developed PTFs
271 to accurately predict K_s , and also revealed the shortcomings of the well-known PTFs. The R^2
272 of the derived over the tested PTFs was observed to be highest for Model 1 in the SDG, and
273 Model 4 in both PFA and PA, and lowest for Model 5 in all three soils. It was observed that
274 the inclusion of exchangeable Ca and Na as predictors increased the predictability of the
275 derived PTFs. Thus, inclusion of additional soil parameters which influence soil aggregation
276 and structure improved the prediction accuracy of the derived PTFs. Another alternative
277 could be the development of soil class specific PTF models.
278

279 REFERENCES

- 280 [1]. Sobieraj JA, Elsenbeer H, Vertessy RA. Pedotransfer functions for estimating saturated
281 hydraulic conductivity: implications for modeling storm flow generation. *J. Hydrol.* 2001;
282 251 (3-4): 202-220.
- 283 [2]. Tuffour HO. Physically based modelling of water infiltration with soil particle phase.
284 Ph.D. Dissertation, Kwame Nkrumah University of Science and Technology, Ghana.
285 2015.
- 286 [3]. Yao RJ, Yang JS, Wu DH, Li FR, Gao P, Wang XP. Evaluation of pedotransfer
287 functions for estimating saturated hydraulic conductivity in coastal salt-affected mud
288 farmland. *J. Soils Sed.* 2015; 15: 902-916.
- 289 [4]. Zhao C, Shao M, Jia X, Nasir M, Zhang C. Using pedotransfer functions to estimate
290 soil hydraulic conductivity in the Loess Plateau of China. *Catena* 2016; 143: 1-6.
- 291 [5]. Cornelis WM, Ronsyn J, Van Meirvenne M, Hartmann R. Evaluation of pedotransfer
292 functions for predicting the soil moisture retention curve. *Soil Sci. Soc. Am. J.* 2001; 65:
293 638-648.
- 294 [6]. Aimrun W, Amin MSM, Eltaib SM. Effective porosity of paddy soils as an
295 estimation of its saturated hydraulic conductivity. *Geoderma* 2004; 121: 197-203.
- 296 [7]. Langhans C, Govers G, Diels J, Clymans W, Van Den Putte A. Dependence of
297 effective hydraulic conductivity on rainfall intensity: loamy agricultural soils. *Hydrol.*
298 *Proc.* 2010; 24 (16): 2257-2268.
- 299 [8]. Saxton, KE, Rawls WJ. Soil water characteristic estimates by texture and organic
300 matter for hydrologic solutions. *Soil Sci. Soc. Am. J.* 2006; 70: 1569-1578.
- 301 [9]. Schaap MG, Leij FJ, van Genuchten MTh. Rosetta: A Computer Program for
302 Estimating Soil Hydraulic Parameters with Hierarchical Pedotransfer Functions. *J.*
303 *Hydrol.* 2001; 251 (3-4): 163-176.
- 304 [10]. Minasny B, Mcbratney AB. Evaluation and development of hydraulic conductivity
305 pedotransfer functions for Australian soil. *Aust. J. Soil Res.* 2000; 38: 905-926.
- 306 [11]. Schaap MG. Rosetta Version 1.0. US Salinity Laboratory, USDA, ARS: Riverside, CA.,
307 1999. <http://www.usssl.ars.usda.gov/models/rosetta/rosetta.htm>. (Accessed:
308 24/06/2017).
- 309 [12]. Carsel RF, Parrish RS. Developing joint probability distributions of soil water retention
310 characteristics. *Water Res. Res.* 1988; 20: 682-690.
- 311 [13]. Wösten JHM, Finke PA, Jansen MJW. Comparison of class and continuous
312 pedotransfer functions to generate soil hydraulic characteristics. *Geoderma* 1995; 66:
313 227-237.
- 314 [14]. Leij FJ, Alves WJ, van Genuchten MTh, Williams JR. The UNSODA unsaturated soil
315 hydraulic database, version 1.0, EPA Report EPA/600/R-96/095, EPA National Risk
316 Management Laboratory, G-72, Cincinnati, OH, USA, 1996.
317 <http://www.usssl.ars.usda.gov/MODELS/UNSODA.HTM> (Accessed: 24/06/2017)

- 318 [15]. Miller EE, Miller RD. Physical theory for capillary flow phenomena. *J. App. Phy.* 1956;
319 27: 324-264.
- 320 [16]. Obiero JPO. Pedotransfer functions for saturated hydraulic conductivity for surface
321 runoff modelling. Ph.D. Thesis, Department of Environmental and Biosystems
322 Engineering, University of Nairobi, Kenya. 2013.
- 323 [17]. Hodnett MG, Tomasella J. Marked differences between van Genuchten soil water-
324 retention parameters for temperate and tropical soils: a new water-retention pedo-
325 transfer functions developed for tropical soils. *Geoderma* 2002; 108: 155-180.
- 326 [18]. Tomasella J, Hodnett MG, Rossato L. Pedotransfer functions for the estimation of soil
327 water retention in Brazilian soils. *Soil Sci. Soc. Am. J.* 2000; 64: 327-338.
- 328 [19]. Rawls WJ, Brakensiek DL. Prediction of soil water properties for hydrologic modeling.
329 In: Jones, EB, Ward TJ. (Eds.) *Watershed Management in the eighties*. Proc. Irrigation
330 and Drainage Division, ASCE Denver, CO., 1985; 293-299.
- 331 [20]. Vereecken H, Maes J, Feyen J, Darius P. Estimating the soil moisture retention
332 characteristic from texture, bulk density, and carbon content. *Soil Sci.* 1989; 148: 389-
333 403.
- 334 [21]. Rawls WJ, Ahuja LR, Brakensiek DL. Estimating soil hydraulic properties from soils
335 data. In: van Genuchten MTh et al. (Eds.). *Indirect methods for estimating the hydraulic*
336 *properties of unsaturated soils*. Proceedings Int. Workshop, Riverside, CA Oct. 11-13.
337 1989. University of California, Riverside, CA., 1992; 329-340.
- 338 [22]. Williams RD, Ahuja LR, Naney JW. Comparison of methods to estimate soil water
339 characteristics from limited texture, bulk density, and limited data. *Soil Sci.* 1992; 153:
340 172-184.
- 341 [23]. Culley JLB. Density and compressibility. In: Carter MR. (Ed.). *Soil Sampling and*
342 *Methods of Analysis*. Canadian Society of Soil Science, Lewis Publishers, CRC Press,
343 Boca Raton, FL., 1993; 529-539.
- 344 [24]. van Genuchten MTh. A Closed-Form Equation for Predicting the Hydraulic Conductivity
345 of Unsaturated Soils. *Soil Sci. Soc. Am. J.* 1980; 44 (5): 892-898.
- 346 [25]. Brakensiek DL, Rawls WJ, Stephenson GR. Modifying SCS hydrologic soil groups and
347 curve numbers for rangeland soils. ASAE paper no. PNR-84203, St. Joseph, MI. 1984.
- 348 [26]. Bonsu M, Laryea KB. Scaling the saturated hydraulic conductivity of an Alfisol. *J. Soil*
349 *Sci.* 1989; 40: 731-742.
- 350 [27]. Tuffour HO, Bonsu M, Abubakari A, Bashagaluke JB, Opoku MA, Oppong JC. Scaling
351 of infiltration rate using the similar media theory and dimensional analysis. *Eura. J. Soil*
352 *Sci.* 2018; 7(4): 308-317.
- 353 [28]. Puckett WE, Dane JH, Hajek BF. Physical and mineralogical data to determine soil
354 hydraulic properties. *Soil Sci. Soc. Am. J.* 1985; 49: 831-836.
- 355 [29]. Campbell GS, Shiozawa S. Prediction of hydraulic properties of soils using particle size
356 distribution and bulk density data. In: van Genuchten MTh et al. (Eds.). *Proceedings of*
357 *the International Workshop on Indirect Methods for Estimating the Hydraulic Properties*
358 *of Unsaturated Soils*. University of California Riverside, Riverside, CA., 1994; 317-328.
- 359 [30]. Dane JH, Puckett W. Field soil hydraulic properties based on physical and
360 mineralogical information. In: van Genuchten MTh et al. (Eds.). *Proceedings of the*
361 *International Workshop on Indirect Methods for Estimating the Hydraulic Properties of*
362 *Unsaturated Soils*, University of California Riverside, Riverside, CA, 1994; 389-403.
- 363 [31]. Ferrer-Julià M, Estrela Monreal T, Sánchez Del Corral Jiménez A, García Meléndez E.
364 Constructing a saturated hydraulic conductivity map of Spain using pedotransfer
365 functions and spatial prediction. *Geoderma* 2004; 123: 275-277.
- 366 [32]. Agyare WA, Park WA, Vlek PLG. Artificial neural network estimation of saturated
367 hydraulic conductivity. *Vadose Zone J.* 2007; 6: 423-431.
- 368 [33]. Pringle MJ, Lark RM. Scale- and location-dependent correlations of soil strength and
369 the yield of wheat. *Soil Till. Res.* 2007; 95: 47-60.
- 370 [34]. Pringle MJ, Romano N, Minasny B, Chirico GB, Lark RM. Spatial evaluation of
371 pedotransfer functions using wavelet analysis. *J. Hydrol.* 2007; 333: 182-198.
- 372 [35]. Tomasella J, Pachepsky YA, Crestana S, Rawls WJ. Comparison of Two Techniques
373 to Develop Pedotransfer Functions for Water Retention. *Soil Sci. Soc. Am. J.* 2003; 67:
374 1085-1092.

- 375 [36]. Wösten JHM, Lilly A, Nemes A Le Bas C. Development and use of a database of
376 hydraulic properties of European soils. *Geoderma* 1999; 90: 169-185.
- 377 [37]. Rasoulzadeh A. Estimating Hydraulic Conductivity Using Pedotransfer Functions,
378 Hydraulic Conductivity-Issues, Determination and Applications. In: Elango L (Ed.).
379 ISBN: 978-953-307-288-3, InTech.
- 380 [38]. Bloemen GW. Calculation of hydraulic conductivities of soils from texture and organic
381 matter content. *Z. Pflanzenernaehr. Bodenk* 1980; 143 (5): 581-615.
- 382 [39]. Jabloun M, Sahli A. Development and comparative analysis of pedotransfer functions
383 for predicting soil water characteristic content for Tunisian soil. *Proceedings of the 7th*
384 *Edition of TJASSST*. 2006; 170-178.
- 385 [40]. Wang Y, Shao M, Liu Z. Pedotransfer Functions for Predicting Soil Hydraulic Properties
386 of the Chinese Loess Plateau. *Soil Sci*. 2012; 177: 424-432.
- 387 [41]. Wagner B, Tarnawski VR, Hennings V, Müller U, Wessolek G, Plagge R. Evaluation of
388 pedo-transfer functions for unsaturated soil hydraulic conductivity using an independent
389 data set. *Geoderma* 2001; 102: 275-297.
- 390 [42]. Ghorbani Dashtaki Sh, Homae M, Khodaverdilo H. Derivation and validation of
391 pedotransfer functions for estimating soil water retention curve using a variety of soil
392 data. *Soil Use Man*. 2010; 26: 68-74.
- 393 [43]. Khodaverdilo H, Homae M, van Genuchten MTh, Ghorbani Dashtaki S. Deriving and
394 validating pedotransfer functions for some calcareous soils. *J. Hydrol*. 2011; 399: 93-
395 99.
- 396 [44]. Jarvis NJ, Zavattaro L, Rajkai K, Reynolds WD, Olsen P-A, McGechan M, Mecke M,
397 Mohanty B, Leeds-Harrison PB, Jacques D. Indirect estimation of near-saturated
398 hydraulic conductivity from readily available soil information. *Geoderma* 2002; 108: 1-
399 17.
- 400 [45]. Li Y, Chen D, White RE, Zhu A, Zhang J. Estimating soil hydraulic properties of
401 Fengqiu County soils in the North China Plain using pedotransfer functions. *Geoderma*
402 2007; 138: 261-271.
- 403 [46]. Haghverdi A, Öztürk HS, Ghosi S, Tunçay T. Estimating saturated hydraulic
404 conductivity using different well-known pedotransfer functions. In: Newton I, Einstein A.
405 (Eds.). *Instructions for Short Papers for the Agro Environ Conference, Wageningen*.
406 2012.
- 407 [47]. Tamari S, Wösten JHM, Ruiz-Suarez JC. Testing an artificial neural network for
408 predicting soil hydraulic conductivity. *Soil Sci. Soc. Am. J*. 1996; 60: 172-1741.
- 409 [48]. Willmott CJ. On the validation of models. *Phys. Geogr*. 1981; 2: 184-194.
- 410 [49]. Candemir F, Gülser C. Influencing factors and prediction of hydraulic conductivity in
411 fine textured alkaline soils. *Arid Land Res. Man*. 2012; 26(1): 15-31.
- 412 [50]. Nemes A, Schaap MG, Wösten JHM. Functional evaluation of pedotransfer functions
413 derived from different scales of data collection. *Soil Sci. Soc. Am. J*. 2003; 67: 1093-
414 1102.

415 **COMPETING INTERESTS**

417 Authors have declared that no competing interests exist.